Biochimica et Biophysica Acta 1827 (2013) 745–750

Contents lists available at SciVerse ScienceDirect

Biochimica et Biophysica Acta

journal homepage: www.elsevier.com/locate/bbabio

Relative importance of driving force and electrostatic interactions in the reduction of multihaem cytochromes by small molecules

Pedro O. Quintas [a], Andreia P. Cepeda [a], Nuno Borges [a], Teresa Catarino [a,b,*], David L. Turner [a]

[a] Instituto de Tecnologia Química e Biológica, Universidade Nova de Lisboa, Av. da República, 2780-157 Oeiras, Portugal
[b] Departamento de Química, Faculdade de Ciências e Tecnologia, FCT, Universidade Nova de Lisboa, 2829-516 Caparica, Portugal

ARTICLE INFO

Article history:
Received 16 November 2012
Received in revised form 8 February 2013
Accepted 12 February 2013
Available online 18 February 2013

Keywords:
Electron transfer
Multihaem cytochromes
Driving force
Electrostatics
Ionic strength
Reduction kinetics

ABSTRACT

Multihaem cytochromes are essential to the energetics of organisms capable of bioremediation and energy production. The haems in several of these cytochromes have been discriminated thermodynamically and their individual rates of reduction by small electron donors were characterized. The kinetic characterization of individual haems used the Marcus theory of electron transfer and assumed that the rates of reduction of each haem by sodium dithionite depend only on the driving force, while electrostatic interactions were neglected. To determine the relative importance of these factors in controlling the rates, we studied the effect of ionic strength on the redox potential and the rate of reduction by dithionite of native *Methylophilus methylotrophus* cytochrome *c″* and three mutants at different pH values. We found that the main factor determining the rate is the driving force and that Marcus theory describes this satisfactorily. This validates the method of the simultaneous fitting of kinetic and thermodynamic data in multihaem cytochromes and opens the way for further investigation into the mechanisms of these proteins.

1. Introduction

Organisms that can be used in the biodegradation and bioremediation of contaminated environments are receiving increasing attention. Gram-negative bacteria from the *Geobacter* and *Shewanella* genera have been shown to be able to reduce toxic compounds containing chromium or uranium [1], as well as insoluble compounds containing iron or manganese [2] through dissimilatory metal reduction. Moreover, they are being applied to the production of energy through the development of microbial fuel cells [3]. These organisms produce a large number of multihaem cytochromes [4] that are present in the periplasm and in the outer membrane; they are crucial to the transfer of electrons to the cell exterior. These features are not restricted to Gram-negative bacteria. Recently, a thermophilic Gram-positive organism, *Thermincola potens* JR, was isolated from the anode of a microbial fuel cell operating at 55 °C. Its genome codes for 32 multihaem cytochromes and it was demonstrated that some of them are localised in the cell surface and are involved in dissimilatory metal reduction [5]. Detailed characterization of these cytochromes is therefore essential, not only structurally but also in terms of their thermodynamic and kinetic properties.

The thermodynamic characterization of the redox centres in multihaem cytochromes is complicated, but redox potentials as well as the interactions between haems and with ionizable centres can be determined by following redox titrations using a combination of NMR and UV–visible spectroscopies [6,7]. Kinetic properties have been determined by studying the sodium dithionite reduction of the cytochromes by the stopped-flow method and then using the thermodynamic parameters for the individual haems and the Marcus theory of electron transfer [8] to separate the contributions of the spectroscopically similar haems [9–12]. The simultaneous analysis of data from all experiments, including kinetics, has found significant use in refining the thermodynamic parameters of multihaem cytochromes.

In the kinetic analysis of the reduction of multihaem proteins by small molecules [9], each haem is assigned a reference rate constant, k_0^i, in which the microscopic redox potential of the centre i is set equal to zero. The reference rate constant accounts for the differences in binding, solvent exposure and general electrostatic environment of the haem. The actual rate constants of the microsteps are related to the reference rate constants by a factor γ_i that accounts for the driving force associated with each particular microstep. The value of the driving force depends on the difference in the reduction potential between the electron donor (E_D) and acceptor (E_A), $\Delta G = F(E_D - E_A)$ where F is the Faraday constant.

The factor γ_i is given by Eq. (1)

$$\gamma_i = \exp\left(\frac{E_i F}{2RT}\left(1 + \frac{E_D F}{\lambda} - \frac{E_i F}{2\lambda}\right)\right) \quad (1)$$

in which E_i is the reduction potential of the centre that is being reduced in a particular microstep, E_D is the reduction potential of the electron donor and λ is the reorganisation energy. The derivation of Eq. (1) is given in the

* Corresponding author at: Instituto de Tecnologia Química e Biológica, Universidade Nova de Lisboa, Av. da República, 2780-157 Oeiras, Portugal. Tel.: +351 214469718.
E-mail address: catarino@itqb.unl.pt (T. Catarino).

0005-2728/$ – see front matter © 2013 Elsevier B.V. All rights reserved.
http://dx.doi.org/10.1016/j.bbabio.2013.02.006

supplementary materials. The value λ is assumed to be constant. Other assumptions made in this approach include the intermolecular electron transfer being slow while intramolecular electron transfer is fast on the experiment timescale, and the electron transfer reaction being effectively irreversible and pseudo-first order, which is achieved by using an excess of reducing agent. Crucially, the variation in the rates of the reduction of individual haems as the reduction of the multihaem protein proceeds is ascribed entirely to the variation in the driving force that arises from haem–haem interactions, and haem–proton interactions, which account for their pH dependence. This raises an important question: what part is played by electrostatic interactions between electron transfer partners?

Methylophilus methylotrophus cytochrome *c″* (cyt *c″*) is a monohaem protein that undergoes a spin-state transition on reduction: the haem is coordinated by two histidines in the oxidized form but only one in the reduced form [13,14]. Both the rate of reduction and the redox potential are strongly dependent on pH [15,16]. It has been proposed that the protonation state of one of the haem propionates is responsible for this behaviour. Haem propionates are also involved in the pH dependence of redox potentials (the redox-Bohr effect) observed in multihaem cytochromes [17,18]. However, it is not clear to what extent the decrease in the rate with pH is due to the electrostatic repulsion by the deprotonated propionate [15] or to the observed decrease in the driving force, hence cyt *c″* is an excellent test case.

The ionic strength of a solution influences the rate of reduction through shielding of electrostatic interactions; when the charges of the electron donor and the protein have the same sign, increasing ionic strength leads to an increase in the rate [19,20], and when the charges are opposite the rate decreases [21,22]. Moreover, changing the charge on the protein by varying the pH of the solution may change and even invert the effect [23]. We aim to clarify the relative contributions of the electrostatic interactions between charges on the protein surface and the charge of the electron donor and the effect of changes in driving force by using cyt *c″* as a model.

We have studied the effect of ionic strength on the rate of reduction by dithionite and the reduction potential of native cyt *c″* and three mutants in order to assess the importance of these two factors in the control of the electron transfer rates. The three pH values chosen, in ascending order, have the haem propionates fully protonated, then one haem propionate is deprotonated, and finally the protein becomes negatively charged as the isoelectric point is passed. Two of the three mutants have positive charges close to the exposed haem edge removed and the third is the double mutant. Extrapolation to infinite ionic strength eliminates the electrostatic contribution, thus isolating the effect of driving force.

The interest of this work is twofold. First, it tests the validity of the kinetic model proposed by Catarino and Turner [9] that is being used to extract information about individual haems in multihaem proteins in different systems. As noted above, the kinetic model does not consider changes of the protein charge while it is being loaded with electrons, or at different pH values: this is an important assumption that requires an experimental validation. Second, this study contributes to a better understanding of biological electron transfer in situations where redox proteins interact with small electron donors or acceptors. This improves our knowledge of the molecular mechanisms involved in the bioenergetics of microorganisms that perform dissimilatory metal reduction, with a potential application to the optimization of bioremediation and energy production processes.

2. Materials and methods

2.1. Expression and purification

Recombinant protein was produced using *Escherichia coli* BL21 (DE3) cells co-transformed with plasmids pCDP1 containing the cyt *c″* gene and pEC86 encoding genes involved in the maturation of *c*-type cytochromes [24]. pCDP1 was prepared by inserting the DNA fragment coding for mature cyt *c″* amplified from pHS1 [25] and digested with restriction enzymes NotI and HindIII, into vector pVA203 [26] digested with the same enzymes. Point mutations were obtained using "QuikChange Site-Directed Mutagenesis Kit" from Agilent. The primers used for cloning and mutagenesis are shown in Table S1 of supplementary materials. Growth and purification were performed as previously reported [27].

2.2. Sample preparation

Buffers at different ionic strengths (0.01–0.2 M) were prepared by diluting a concentrated KCl solution in 50 mM acetate buffer pH 4.5, 5 mM phosphate buffer pH 7.7 or 10 mM Glycine buffer pH 10.0; small pH variations were corrected by adding concentrated HCl or KOH. Protein solutions were prepared by diluting a concentrated stock solution in the desired buffer. Dithionite solutions were prepared in the same buffer as the protein for the experiments at pH 7.7 and pH 10.0. For the experiments at pH 4.5, solutions were prepared in 2.5 mM phosphate buffer pH 7.0 to avoid dithionite decomposition in acidic conditions, with KCl added to the desired ionic strength.

2.3. Kinetic experiments

Stopped-flow kinetic experiments were performed at 25 °C using a SF-61 DX2 stopped-flow apparatus (Hi-Tech Scientific) placed inside an anaerobic chamber (<2 ppm O_2). The reaction was initiated by mixing a protein and a dithionite solution (1:1) with the same ionic strength, prepared as above. The change in absorbance at 406 nm (Soret peak in oxidized cyt *c″*) and 426 nm (Soret peak in reduced cyt *c″*) was followed as a function of time.

Protein and dithionite concentrations were determined in every experiment by mixing each solution with the buffer where it was prepared and recording the absorbance at 406 nm and 315 nm, respectively, using the following extinction coefficients: $\varepsilon_{\text{cyt } c'',\ 406\ \text{nm}} = 97.5\ \text{mM}^{-1}\ \text{cm}^{-1}$ [13], and $\varepsilon_{\text{dithionite},\ 315\ \text{nm}} = 8\ \text{mM}^{-1}\ \text{cm}^{-1}$ [28]. The pH values were measured after mixing.

It has been determined previously that the reducing agent is not dithionite but the product of its dissociation, $SO_2^{\bullet-}$ [15]. Despite the very low dissociation constant, the concentration of $SO_2^{\bullet-}$ is practically constant due to the high concentration of dithionite and the very fast rate of dissociation, making the reaction pseudo-first-order [9]. Rate constants k_{obs} were obtained by single exponential fitting to the traces. Second-order rate constants k were obtained as:

$$k = k_{obs}([\text{dithionite}] \times K)^{-\frac{1}{2}} \tag{2}$$

where K is the equilibrium dissociation constant of dithionite. The variation of K with the ionic strength, I, was taken into account via an extended Debye–Hückel equation [29]:

$$\ln K = \ln k_1^{\infty} - \ln k_{-1}^{\infty} + \frac{2Z^2\alpha\sqrt{I}}{1+\kappa R} - \frac{4Z^2\alpha\sqrt{I}}{1+2\kappa R} \tag{3}$$

where $Z = -1$, $\alpha = 1.17\ \text{M}^{-½}$, $\kappa = 0.329\sqrt{I}\ \text{Å}^{-1}$ and $R = 1.5$ Å [30]. We obtain $\ln k_1^{\infty} - \ln k_{-1}^{\infty} = -19.93$ from the data of Thorneley and Lowe by using $I = 0.03$ M and $K = 1.60 \times 10^{-9}$ M [31].

2.4. Redox titrations

Potentiometric titrations were performed inside an anaerobic chamber (<2 ppm O_2) at a constant temperature of 25 °C. Protein samples were prepared as above to a final concentration of 5 μM. Indigo disulfonate, indigo trisulfonate, indigo tetrasulfonate and methylene blue were used as redox mediators, each with a final concentration of 1 μM. The solution potential was measured with a

combined platinum–Ag/AgCl electrode (Crison ref. 52–65) and corrected to the standard hydrogen electrode. Reduction was achieved by adding small volumes of a sodium dithionite solution prepared as above and oxidation was achieved by the addition of air with a gas-tight syringe. The redox state of the protein was monitored by recording the UV–visible spectrum after each addition once a stable potential reading had been attained. Each spectrum was fitted as a sum of the spectra of the pure reduced and oxidized forms to obtain the fractions. The fraction of reduced protein was then plotted against the measured potential and the redox potential was obtained from the fitting of a single electron Nernst curve to the experimental points.

The fit of the ionic strength dependence of the reduction potentials, as well as the extrapolation to infinite ionic strength and the effective charge on the protein, Z_1, were made with Eq. (4) [32]:

$$\Delta E^{\circ} = \Delta E^{\infty} - 0.09182\left(\frac{exp(-\kappa R_1)}{1+\kappa R_2} + \frac{exp(-\kappa R_2)}{1+\kappa R_1}\right)\left(\frac{Z_1 Z_2 - Z_1' Z_2'}{R_1 + R_2}\right) \quad (4)$$

where ΔE° is the reduction potential at ionic strength I, ΔE^{∞} is the reduction potential at infinite ionic strength, Z_1 and Z_2 are the charges and R_1 and R_2 are the radii of the reactants. The primed terms represent the products. The values of the charge and radius of the reducing agent used in the fit were, $Z_2 = -1$, $Z_2' = 0$, and $R_2 = 1.5$ Å [30], and $\kappa = 0.329\sqrt{I}$ Å^{-1} for water at 25 °C. Since the best value for R_1 is unknown, fits were performed with $R_1 = 5$ and 8 Å, which correspond to the distance from the exposed haem edge or haem propionate to the iron, respectively.

3. Results and discussion

The objective of this work is to distinguish the influence of driving force and of electrostatic interactions in the electron transfer reactions between proteins and small molecules. Both the rate of reduction of cyt *c*″ by sodium dithionite and its reduction potential show a strong dependence on pH [15,16], making the protein a suitable model. The overall electron transfer process

$$D^- + A^+ \overset{K_{ass}}{\rightleftharpoons} \left[D^- - A^+\right] \xrightarrow{k_{ET}} [D - A] \overset{K_{diss}}{\rightleftharpoons} D + A$$

can be simplified if the electron transfer is the rate limiting step and the electron transfer is effectively unidirectional. The reaction then becomes:

$$D^- + A^+ \xrightarrow{k} D + A$$

where the second order rate constant of the electron transfer reaction is the product of the equilibrium association constant for the complex formation between electron donor and electron acceptor and the rate constant for electron transfer, $k = K_{ass} \times k_{ET}$ [9]. The rate constant for electron transfer is described by Marcus theory [8] and depends on the driving force among other factors. The driving force is the difference between the reduction potential of the reducing agent $SO_2^{\bullet -}$ [15], which is constant and equal to −0.30 V [33], and the reduction potential of the cyt *c*″, which depends on pH and ionic strength. The reduction potential of cyt *c*″ was determined from redox titrations followed by visible spectroscopy. The ionic strength dependence of the reduction potentials of the native cytochrome c″ at pH 4.5 and 7.7 was fitted with Eq. (4) to obtain the reduction potentials at infinite ionic strength and the results are shown in Fig. 1.

These data show that the value of E° at pH 7.7 is about 120 mV lower than that at pH 4.5. Also, the reduction potential increases with the ionic strength at pH 7.7, whereas the dependence on ionic strength is small at pH 4.5. This difference can be explained by the influence of the haem propionate group that is protonated at pH 4.5 and deprotonated at pH 7.7. The negative charge of the deprotonated propionate makes it more difficult to reduce the iron at pH 7.7, so that the reduction potential decreases with respect to that at pH 4.5, and partial shielding of the propionate charge would cause the increase in the reduction potential with ionic strength.

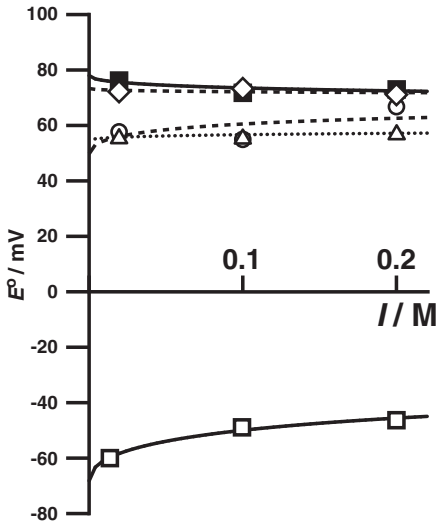

Fig. 1. Dependence of the reduction potential, E°, of cyt *c*″ on the ionic strength, *I*, at pH 7.7 (WT — open squares, solid line) and pH 4.5 (WT — filled squares, solid line; K80Q — open circles, dashed line; K68Q — open diamonds, dashed line; K68/80Q — open triangles, dotted line). The lines are the result of the fit of Eq. (4) to the data points. The values of the reduction potentials extrapolated to infinite ionic strength were obtained from the fit.

To investigate the role played by electrostatic interactions, the rate of reduction of cyt *c*″ by sodium dithionite was studied at pH 4.5, 7.7 and 10.0, as a function of ionic strength. The second order rate constants obtained are presented in Table 1. These values show that the rate constant of the reaction decreases with increasing pH, as observed before [15]. The change from pH 4.5 to pH 7.7 can be explained by the decrease in driving force and/or increase in repulsive interactions (or decrease in attractive interactions) due to the deprotonation of the haem propionate. There is little change in the reduction potential between pH 7.7 and pH 10 [16] but the overall charge on the protein becomes negative since pH 10 is well above the isoelectric point of 8.7 [13].

The decimal logarithmic plot of the relative rate constants as a function of the square root of the ionic strength is shown in Fig. 2: a positive slope indicates repulsive interactions, a negative slope indicates attractive interactions, and a slope equal to zero shows that there are no significant electrostatic interactions. A qualitative understanding of the magnitude of the slope is given by the equation of the Debye–Hückel Limiting Law, $log\ (k/k_0) = 1.02\ Z_1 Z_2\ \sqrt{I}$ [34] that shows that the slope is proportional to the product of the interacting charges. Because the rate constants decrease when the shielding of the interacting charges increases, Fig. 2 shows that this reaction is influenced by attractive

Table 1
Second order rate constants (/10^8 s^{-1} M^{-1}) for the reduction of cyt *c*″ with sodium dithionite.

I (mM)	pH 4.5	pH 7.7	pH 10
19.5	7.59	1.57[a]	0.882[b]
30	7.07	1.52	0.875[c]
50	6.09	1.41	0.918
100	5.07	1.25	0.912
150	4.29	1.18	0.913
200	3.76	1.11	0.872

[a] I = 13.4 mM.
[b] I = 7 mM.
[c] I = 20 mM.

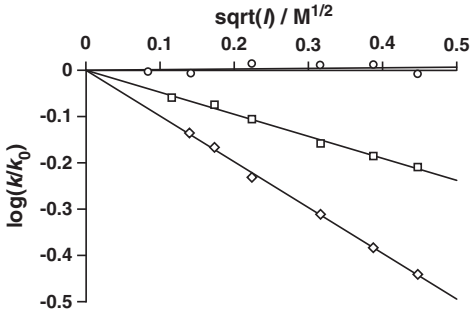

Fig. 2. Dependence of $log(k/k_0)$ on the square root of the ionic strength at different pH values (diamonds pH 4.5, squares pH 7.7 and circles pH 10.0); k_0 is the rate constant extrapolated to zero ionic strength.

electrostatic interactions. It should be noted that the negative slopes are not an effect of driving force because the driving force for electron transfer is practically independent of ionic strength at pH 4.5, and at pH 7.7 it actually increases. Since the reducing agent is negatively charged, this implies interactions with positive charges on the protein. Moreover, since the slope is close to zero at pH 10, these data demonstrate clearly that the overall charge of the protein is not the deciding factor. Since the distribution of charge at pH 10 is not known, this pH will not be considered further. As noted above, the major change between pH 4.5 and pH 7.7 is the deprotonation of a haem propionate, and the effective charge on the protein clearly becomes less positive. The slope decreases by about 0.5 units in response to the unit change in the propionate charge, which again shows that the dependence cannot be described by the Debye Hückel Limiting Law with the overall protein charge.

The electrostatic potential on the surface of cyt *c*″ calculated by APBS [35] at pH 4.5 and pH 7.7 is presented in Fig. 3: a region near the exposed haem edge is positively charged (blue) at both pH values despite having a negatively charged propionate at pH 7.7. This region includes Arg81, Lys80 and Lys68 and is a likely region for the access of $SO_2^{\bullet-}$ to the haem.

The lysine residues K68 and K80 were replaced by glutamine, which is also polar but not charged, and the reduction potentials and kinetics of reduction by sodium dithionite of the mutants K68Q, K80Q and double mutant K68/80Q were studied at pH 4.5 as a function of ionic strength. This study was performed at pH 4.5 to avoid interference from the deprotonation of the haem propionates, which might have different pK_a values in the mutants. Hence, the introduction of a negative charge on the propionate at pH 7.7 may be compared with the removal of two positive charges close to the haem at pH 4.5. The results obtained are presented in Table 2 and Fig. 4. As can be seen in Fig. 1, replacing lysine 68, has a negligible effect on the reduction potential of cyt *c*″ whereas the substitution of lysine 80 by glutamine leads to ca. 15 mV decrease, and the effect of the double mutant is similar. These effects are small by comparison with the effect of deprotonating the haem propionate at pH 7.7, that shifts the reduction potential by 120 mV. The distance from the nitrogen of the ε-amino group in K68 to the haem iron is 12.9 Å in the oxidized crystal structure [39] and the distance from K80 to the haem iron is 18.3 Å, both of which are much larger than the 7.8 Å between the carboxylate group of the propionate and the haem iron. The differences decrease further at higher ionic strengths, and extrapolation to infinite ionic strength gives similar values of the reduction potentials for the wild type and the mutants.

As expected, the second order rate constants obtained for the mutants (Table 2) are smaller than those obtained at pH 4.5 for the wild type cytochrome (Table 1) because the removal of a positively charged residue should decrease the attractive electrostatic interaction between the negatively charged reducing agent and the protein. The mutation of K68 has a significantly larger effect on the rate constant, both on its absolute value (Table 2) and on its ionic strength dependence (Fig. 4), suggesting that the access route of $SO_2^{\bullet-}$ to the haem is closer to lysine 68 than to lysine 80. The effect of the double mutation on the rate constant is roughly equal to the sum of the effects of the two single mutants and is significantly smaller than the effect of deprotonating the haem propionate at pH 7.7 (compare Tables 1 and 2 and Figs. 2 and 4).

We have demonstrated that positive electrostatic interactions do play a role in the reduction of cyt *c*″ by sodium dithionite and that electron transfer is likely to occur with $SO_2^{\bullet-}$ close to the exposed haem edge. To assess the relative contribution of driving force it is necessary to compare the rate constants at infinite ionic strength, so that the electrostatic interactions can be eliminated. A suitable model for this extrapolation is obtained from Marcus theory applied to the Debye–Hückel formalism [40]:

$$\ln k = \ln k_\infty - 3.576\left(\frac{\exp(-\kappa R_1)}{1+\kappa R_2} + \frac{\exp(-\kappa R_2)}{1+\kappa R_1}\right)\left(\frac{Z_1 Z_2}{R_1 + R_2}\right) \quad (5)$$

where k is the rate constant at ionic strength I, k_∞ is the rate constant at infinite ionic strength, $\kappa = 0.329\sqrt{I}$ Å^{-1} at 25 °C, and the Z_i and R_i are the charges and radii of the two reactants.

Eq. (5) can be used to fit the experimental data and obtain values for k_∞, the rate constant at infinite ionic strength, and Z_1, the charge on the protein surface that is relevant for the electron transfer reaction. The values of $Z_2 = -1$, $R_2 = 1.5$ Å and $R_1 = 5$ or 8 Å were the same that were used in Eq. (4). The result of the fits is presented in Fig. S1 of

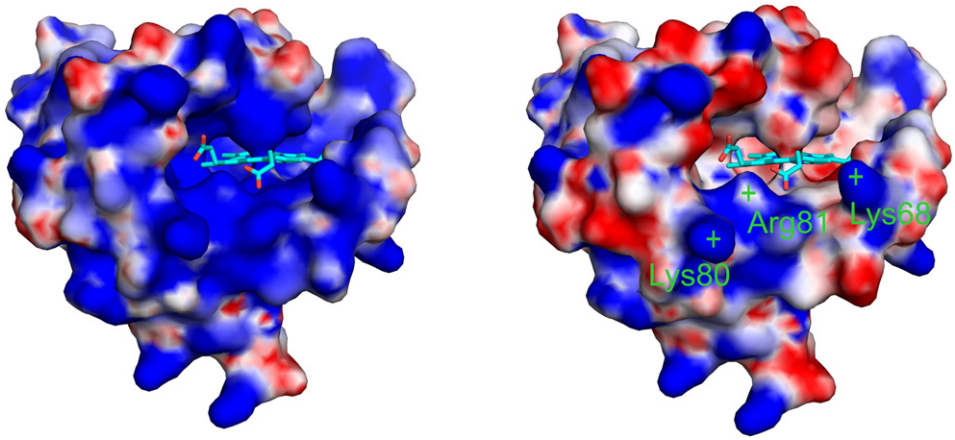

Fig. 3. Electrostatic potential on the surface of cyt *c*″ (PDB ID: 1GU2) at pH 4.5 (left) and pH 7.7 (right), calculated by APBS [35]. Blue corresponds to a positive charge and red to a negative charge. Prediction of pK_a values by PropKa [36] and preparation of structure for electrostatic calculations by PDB2PQR) [37]. The figures were prepared with PyMOL [38].

Table 2
Second order rate constants (/10^8 s^{-1} M^{-1}) for the reduction of cyt *c*″ mutants K68Q, K80Q and K68/80Q with sodium dithionite at pH 4.5.

I (mM)	K80Q	K68Q	K68/80Q
19.5	7.10	5.72	5.21
30	6.29	5.48	4.54
50	5.58	5.82	4.38
100	4.38	3.95	3.62
150	3.92	3.54	3.20
200	3.57	3.13	2.84

supplementary materials. The values of the charge determined from the fit are presented in Table 3 and the values of the rate constants at infinite ionic strength are given in Table 4.

For the wild type protein, values of the protein charge, Z_1, of approximately +2 and +1 were obtained for pH 4.5 and pH 7.7, respectively. These values are plausible, taking into account the positive charges of the nearby amino acids and the neutral haem propionate that becomes negatively charged at pH 7.7. In the single mutants there is a decrease in the calculated charge at pH 4.5, albeit a fraction of the +1 charge of the lysines. It is also noticeable that the effect of the mutation of lysine 68 on the charge is significantly larger than that of lysine 80. Moreover, the effect of the mutations seems to be roughly additive. The effect of the mutations on the rate constant at infinite ionic strength is small, which is in agreement with the small change in the reduction potentials of the mutants when compared to the wild type cytochrome.

Marcus theory for electron transfer [8] can be used to calculate the change in the electron transfer rate k_{ET} expected for a given change in driving force, if it is assumed that the reorganisation energy λ and the pre-exponential term do not change. Under these conditions, Eq. (6) can be used to calculate the ratio between the electron transfer rates at pH 4.5 and 7.7. Note that, when the reduction potentials, E_{cytc}, are ionic strength dependent, as it is in the case at pH 7.7 (see Fig. 1), the values used in Eq. (6) should be the values extrapolated for infinite ionic strength.

$$\frac{k_{ET}^{pH\ 4.5}}{k_{ET}^{pH\ 7.7}} = \exp\left(\frac{\left(E_{cytc}^{pH\ 4.5} - E_{cytc}^{pH\ 7.7}\right)F}{2RT}\left(1 + \frac{E_{SO2}F}{\lambda} - \frac{\left(E_{cytc}^{pH\ 4.5} + E_{cytc}^{pH\ 7.7}\right)F}{2\lambda}\right)\right). \quad (6)$$

The reduction potential of the electron donor, E_{SO2}, is −0.30 V and is pH independent in this pH range [33]. A value of 0.7 eV was used for the reorganisation energy λ [41].

The ratio of the second order rate constants, extrapolated to infinite ionic strength to cancel out electrostatic contributions (Table 4), and the ratio of the rate constants calculated with Eq. (6) using the reduction potentials of the cytochrome, also extrapolated to infinite ionic strength, are presented in Table 5. The agreement is reasonable,

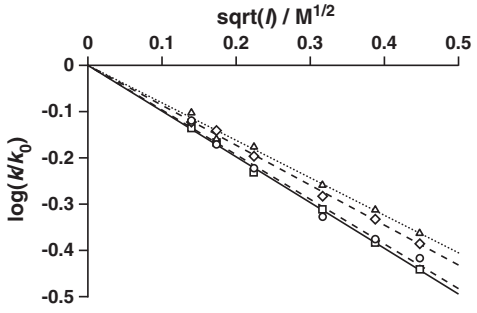

Fig. 4. Dependence of $log(k/k_0)$, the relative rates, on the square root of the ionic strength at pH 4.5. Comparison between native cyt *c*″ (squares, solid line) and mutants K80Q (circles, dashed line), K68Q (diamonds dashed line), and K68/80Q (triangles, dotted line).

Table 3
Effective protein charge, Z_1, obtained via Eq. (5).

R_1 (Å)	Wild type		K80Q	K68Q	K68/80Q
	pH 4.5	pH 7.7	pH 4.5	pH 4.5	pH 4.5
5	+1.95 ± 0.08	+0.91 ± 0.06	+1.92 ± 0.04	+1.70 ± 0.07	+1.60 ± 0.10
8	+2.60 ± 0.14	+1.20 ± 0.10	+2.56 ± 0.05	+2.27 ± 0.12	+2.12 ± 0.16

showing that the driving force influences the rate of reduction of cyt *c*″ by sodium dithionite according to the predictions of Marcus theory and this set of assumptions.

4. Conclusions

This work addresses the contributions of electrostatic interactions and driving force to the electron transfer rates by studying the ionic strength dependence of the reduction of cyt *c*″ by sodium dithionite at different pH values. The thermodynamic modulation of electron transfer rates is adequately described by Marcus theory for electron transfer, assuming a constant value for the reorganisation energy. The studies with ionic strength showed that the region on the protein surface that is involved in the electrostatic interaction between the redox partners is positively charged and probably involves the exposed haem edge. This was tested further by single-site mutagenesis and it was concluded that the approach of the reducing agent to the haem is closer to lysine 68 than to lysine 80. The protonation state of one of the haem propionates influences the rate of reduction both by changing the reduction potential and through electrostatic repulsion. The importance of the haem propionates has also been observed in the reduction of cytochrome b_5 [42] and myoglobin [43,44]. In both cases, esterification of the propionates results in an increase in the redox potential and the rate of reduction.

In some previous studies on the ionic strength dependence of the redox potential and the rate of electron transfer, with a similar treatment to that used here, the full radius of the protein was used in the calculations and the values of the charges that were obtained were usually somewhat different from the expected full charge of the protein [20,22,45]. This is particularly evident with cyt *c*″ because reversing the charge of the protein by using a pH above the isoelectric point does not reverse the interaction between the protein and the reducing agent. Therefore, the effective radius appears to be more closely related to the region of accessibility of the haem to the reducing agent.

At a typical ionic strength of ca. 50 mM, the experimental rate of reduction decreases by a factor of 4.3 between pH 4.5 and pH 7.7. This may be compared with the factor of 4.0 calculated from Marcus theory solely on the basis of the change in driving force (for I = 50 mM, $E^{pH\ 4.5} = 74$ mV, $E^{pH\ 7.7} = -54$ mV). Clearly, the effect of driving force is dominant in this case, though electrostatic interactions also play a part. This helps to explain the success of the simultaneous fitting of kinetic and thermodynamic data in multihaem cytochromes over a wide pH range [11]: variations in surface charge have a limited effect, and even changing the charge of a haem propionate has less effect on the electrostatic interaction with dithionite than it does on the driving force through redox-Bohr effects. Furthermore, the ionisation of the propionate of one haem in a multihaem protein is not likely to affect the rate of reduction of a different

Table 4
Rate constants for reduction of cyt *c*″ at infinite ionic strength (/10^8 s^{-1} M^{-1}).

R_1 (Å)	Wild type		K80Q	K68Q	K68/80Q
	pH 4.5	pH 7.7	pH 4.5	pH 4.5	pH 4.5
5	1.54 ± 0.08	0.73 ± 0.03	1.44 ± 0.04	1.44 ± 0.06	1.38 ± 0.09
8	2.13 ± 0.11	0.86 ± 0.03	1.97 ± 0.04	1.91 ± 0.09	1.80 ± 0.11

Table 5
Reduction potentials at infinite ionic strength used with Eq. (6) to calculate the ratio of ET rate constants according to Marcus theory. The ratios are compared with the ratio of experimental second order rate constants extrapolated to infinite ionic strength (values from Table 4). A value of $\lambda = 0.7$ eV was used in the calculations [41].

R_1 (Å)	E_{cytc} (mV)		$k_{ET}^{pH\ 4.5}/k_{ET}^{pH\ 7.7}$	
	pH 4 5	pH 7.7	From Eq. (6)	From Table 4
5	68	−29	2.8	2.1 ± 0.2
8	70	−35	3.1	2.5 ± 0.2

haem through electrostatic interactions, since this work also showed that the influence of charges on the protein surface is limited to a restricted area in the vicinity of the redox centre. Hence, the crucial assumption made in the method for kinetic and thermodynamic analysis of multihaem proteins, that electrostatic interactions between the protein and dithionite may be neglected, has a sound experimental basis.

Acknowledgements

This work was supported by PTDC/QUI/65640/2006, and Ph.D. Grant SFRH/BD/36716/2007 (to P.O.Q.). Plasmid pVA203 was a kind gift from Prof. Carlos A. Salgueiro fom FCT/UNL. We thank Dr. Luís G. Gonçalves for helpful suggestions.

Appendix A. Supplementary data

Supplementary data to this article can be found online at http://dx.doi.org/10.1016/j.bbabio.2013.02.006.

References

[1] R.T. Anderson, H.A. Vrionis, I. Ortiz-Bernad, C.T. Resch, P.E. Long, R. Dayvault, K. Karp, S. Marutzky, D.R. Metzler, A. Peacock, D.C. White, M. Lowe, D.R. Lovley, Stimulating the in situ activity of *Geobacter* species to remove uranium from the groundwater of a uranium-contaminated aquifer, Appl. Environ. Microbiol. 69 (2003) 5884–5891.
[2] K.H. Nealson, D. Saffarini, Iron and manganese in anaerobic respiration: environmental significance, physiology, and regulation, Annu. Rev. Microbiol. 48 (1994) 311–343.
[3] B.E. Logan, Exoelectrogenic bacteria that power microbial fuel cells, Nat. Rev. Microbiol. 7 (2009) 375–381.
[4] J.K. Fredrickson, M.F. Romine, A.S. Beliaev, J.M. Auchtung, M.E. Driscoll, T.S. Gardner, K.H. Nealson, A.L. Osterman, G. Pinchuk, J.L. Reed, D.A. Rodionov, J.L. Rodrigues, D.A. Saffarini, M.H. Serres, A.M. Spormann, I.B. Zhulin, J.M. Tiedje, Towards environmental systems biology of *Shewanella*, Nat. Rev. Microbiol. 6 (2008) 592–603.
[5] H.K. Carlson, A.T. Iavarone, A. Gorur, B.S. Yeo, R. Tran, R.A. Melnyk, R.A. Mathies, M. Auer, J.D. Coates, Surface multiheme c-type cytochromes from *Thermincola potens* and implications for respiratory metal reduction by Gram-positive bacteria, Proc. Natl. Acad. Sci. U. S. A. 109 (2012) 1702–1707.
[6] C.A. Salgueiro, D.L. Turner, H. Santos, J. LeGall, A.V. Xavier, Assignment of the redox potentials to the four haems in *Desulfovibrio vulgaris* cytochrome c_3 by 2D-NMR, FEBS Lett. 314 (1992) 155–158.
[7] M. Pessanha, L. Morgado, R.O. Louro, Y.Y. Londer, P.R. Pokkuluri, M. Schiffer, C.A. Salgueiro, Thermodynamic characterization of triheme cytochrome PpcA from *Geobacter sulfurreducens*: evidence for a role played in e^-/H^+ energy transduction, Biochemistry 45 (2006) 13910–13917.
[8] R.A. Marcus, N. Sutin, Electron transfers in chemistry and biology, Biochim. Biophys. Acta 811 (1985) 265–322.
[9] T. Catarino, D.L. Turner, Thermodynamic control of electron transfer rates in multicentre redox proteins, ChemBioChem 2 (2001) 416–424.
[10] I.J. Correia, C.M. Paquete, R.O. Louro, T. Catarino, D.L. Turner, A.V. Xavier, Thermodynamic and kinetic characterization of trihaem cytochrome c(3) from *Desulfuromonas acetoxidans*, Eur. J. Biochem. 269 (2002) 5722–5730.
[11] C.M. Paquete, D.L. Turner, R.O. Louro, A.V. Xavier, T. Catarino, Thermodynamic and kinetic characterisation of individual haems in multicentre cytochromes c_3, Biochim. Biophys. Acta 1767 (2007) 1169–1179.
[12] Y. Qian, C.M. Paquete, R.O. Louro, D.E. Ross, E. LaBelle, D.R. Bond, M. Tien, Mapping the iron binding site(s) on the small tetraheme cytochrome of *Shewanella oneidensis* MR-1, Biochemistry 50 (2011) 6217–6224.
[13] H. Santos, D.L. Turner, Characterization and NMR studies of a novel cytochrome *c* isolated from *Methylophilus methylotrophus* which shows a redox-linked change of spin state, Biochim. Biophys. Acta 954 (1988) 277–286.
[14] H.S. Costa, H. Santos, D.L. Turner, Characterization of the haem environment in *Methylophilus methylotrophus* ferricytochrome *c″* by ^{1}H NMR, Eur. J. Biochem. 215 (1993) 817–824.
[15] M. Coletta, H. Costa, G. De Sanctis, F. Neri, G. Smulevich, D.L. Turner, H. Santos, pH dependence of structural and functional properties of oxidized cytochrome *c″* from *Methylophilus methylotrophus*, J. Biol. Chem. 272 (1997) 24800–24804.
[16] H.S. Costa, H. Santos, D.L. Turner, A.V. Xavier, Involvement of a labile axial histidine in coupling electron and proton transfer in *Methylophilus methylotrophus* cytochrome *c″*, Eur. J. Biochem. 208 (1992) 427–433.
[17] J.S. Park, T. Ohmura, K. Kano, T. Sagara, K. Niki, Y. Kyogoku, H. Akutsu, Regulation of the redox order of four hemes by pH in cytochrome c_3 from *D. vulgaris* Miyazaki F, Biochim. Biophys. Acta 1293 (1996) 45–54.
[18] D.L. Turner, C.A. Salgueiro, T. Catarino, J. Legall, A.V. Xavier, NMR studies of cooperativity in the tetrahaem cytochrome c_3 from *Desulfovibrio vulgaris*, Eur. J. Biochem. 241 (1996) 723–731.
[19] J.V. McArdle, H.B. Gray, C. Creutz, N. Sutin, Kinetic studies of the oxidation of ferrocytochrome *c* from horse heart and *Candida krusei* by tris(1,10-phenanthroline) cobalt(III), J. Am. Chem. Soc. 96 (1974) 5737–5741.
[20] L.S. Reid, A.G. Mauk, Kinetic analysis of cytochrome b_5 reduction by $Fe(EDTA)^{2-}$, J. Am. Chem. Soc. 104 (1982) 841–845.
[21] H.L. Hodges, R.A. Holwerda, H.B. Gray, Kinetic studies of the reduction of ferricytochrome *c* by $Fe(EDTA)^{2-}$, J. Am. Chem. Soc. 96 (1974) 3132–3137.
[22] A.R. Lim, A.G. Mauk, Kinetic analysis of metsulphmyoglobin and metmyoglobin reduction by $Fe(EDTA)^{2-}$, Biochem. J. 229 (1985) 765–769.
[23] T. Goldkorn, A. Schejter, Electrostatic effects on the kinetics of oxidation–reduction reactions of *c*-type cytochromes, J. Biol. Chem. 254 (1979) 12562–12566.
[24] E. Arslan, H. Schulz, R. Zufferey, P. Kunzler, L. Thony-Meyer, Overproduction of the *Bradyrhizobium japonicum c*-type cytochrome subunits of the cbb_3 oxidase in *Escherichia coli*, Biochem. Biophys. Res. Commun. 251 (1998) 744–747.
[25] N.J. Price, L. Brennan, T.Q. Faria, E. Vijgenboom, G.W. Canters, D.L. Turner, H. Santos, High yield of *Methylophilus methylotrophus* cytochrome *c″* by coexpression with cytochrome *c* maturation gene cluster from *Escherichia coli*, Protein Expr. Purif. 20 (2000) 444–450.
[26] P.R. Pokkuluri, Y.Y. Londer, N.E. Duke, J. Erickson, M. Pessanha, C.A. Salgueiro, M. Schiffer, Structure of a novel c_7-type three-heme cytochrome domain from a multidomain cytochrome *c* polymer, Protein Sci. 13 (2004) 1684–1692.
[27] P.O. Quintas, T. Catarino, S. Todorovic, D.L. Turner, Highly selective ligand binding by *Methylophilus methylotrophus* cytochrome *c″*, Biochemistry 50 (2011) 5624–5632.
[28] M. Dixon, The acceptor specificity of flavins and flavoproteins. I. Techniques for anaerobic spectrophotometry, Biochim. Biophys. Acta 226 (1971) 241–258.
[29] J.C. Chien, L.C. Dickinson, Reduction of cobalticytochrome *c* by dithionite, J. Biol. Chem. 253 (1978) 6965–6972.
[30] R.J. Balahura, M.D. Johnson, Outer-sphere dithionite reductions of metal complexes, Inorg. Chem. 26 (1987) 3860–3863.
[31] R.N. Thorneley, D.J. Lowe, Nitrogenase of *Klebsiella pneumoniae*. Kinetics of the dissociation of oxidized iron protein from molybdenum–iron protein: identification of the rate-limiting step for substrate reduction, Biochem. J. 215 (1983) 393–403.
[32] A.G. Mauk, R.A. Scott, H.B. Gray, Distances of electron-transfer to and from metalloprotein redox sites in reactions with inorganic complexes, J. Am. Chem. Soc. 102 (1980) 4360–4363.
[33] P. Neta, R.E. Huie, A. Harriman, One-electron-transfer reactions of the couple SO_2/SO_2^- in aqueous solutions. Pulse radiolytic and cyclic voltammetric studies, J. Phys. Chem. 91 (1987) 1606–1611.
[34] P.W. Atkins, J. de Paula, Physical Chemistry, 8th ed. Oxford University Press, 2006.
[35] N.A. Baker, D. Sept, S. Joseph, M.J. Holst, J.A. McCammon, Electrostatics of nanosystems: application to microtubules and the ribosome, Proc. Natl. Acad. Sci. U. S. A. 98 (2001) 10037–10041.
[36] H. Li, A.D. Robertson, J.H. Jensen, Very fast empirical prediction and rationalization of protein pKa values, Proteins 61 (2005) 704–721.
[37] T.J. Dolinsky, J.E. Nielsen, J.A. McCammon, N.A. Baker, PDB2PQR: an automated pipeline for the setup of Poisson-Boltzmann electrostatics calculations, Nucleic Acids Res. 32 (2004) W665–667.
[38] The PyMOL Molecular Graphics System, version 0.99rc6, Schrodinger, LLC, 2006.
[39] F.J. Enguita, E. Pohl, D.L. Turner, H. Santos, M.A. Carrondo, Structural evidence for a proton transfer pathway coupled with haem reduction of cytochrome *c″* from *Methylophilus methylotrophus*, J. Biol. Inorg. Chem. 11 (2006) 189–196.
[40] S. Wherland, H.B. Gray, Metalloprotein electron transfer reactions: analysis of reactivity of horse heart cytochrome *c* with inorganic complexes, Proc. Natl. Acad. Sci. U. S. A. 73 (1976) 2950–2954.
[41] M. Sulpizi, S. Raugei, J. VandeVondele, P. Carloni, M. Sprik, Calculation of redox properties: understanding short- and long-range effects in rubredoxin, J. Phys. Chem. B 111 (2007) 3969–3976.
[42] L.S. Reid, M.R. Mauk, A.G. Mauk, Role of heme propionate groups in cytochrome b_5 electron transfer, J. Am. Chem. Soc. 106 (1984) 2182–2185.
[43] K. Tsukahara, K. Ishida, Kinetics and mechanism of reduction of metmyoglobins by dithionite. Role of the heme propionates, Bull. Chem. Soc. Jpn. 64 (1991) 2378–2382.
[44] A.R. Lim, B.P. Sishta, A. Grant Mauk, Contribution of the heme propionate groups to the electron transfer and electrostatic properties of myoglobin, J. Inorg. Biochem. 100 (2006) 2017–2023.
[45] L.S. Reid, V.T. Taniguchi, H.B. Gray, A.G. Mauk, Oxidation–reduction equilibrium of cytochrome b_5, J. Am. Chem. Soc. 104 (1982) 7516–7519.